

# Two-dimensional Penrose-tiled photonic quasicrystals: from diffraction pattern to band structure

M A Kaliteevski<sup>†</sup>, S Brand<sup>†</sup>, R A Abram<sup>†</sup>, T F Krauss<sup>‡</sup>, R DeLa Rue<sup>‡</sup> and P Millar<sup>‡</sup>

<sup>†</sup> Department of Physics, University of Durham, South Road, Durham DH1 3LE, UK

<sup>‡</sup> Department of Electronics and Electrical Engineering, Glasgow University, Glasgow G12 8LT, UK

Received 23 June 2000, in final form 31 July 2000

**Abstract.** We report measurements of the diffraction pattern of a two-dimensional photonic quasicrystal structure and use the set of plane waves defined by the diffraction pattern as the basis of a theoretical approach to calculate the photonic band structure of the system. An important feature of the model is that it retains the essence of the rotational and inflational properties of the quasicrystal at all levels of approximation: properties lost in approximate models which artificially introduce elements of periodicity.

The calculated density of modes of the quasicrystals is found to display a weakly depleted region analogous to the bandgap that occurs in a periodic system. The calculated transmission spectra for different polarizations and directions of propagation show features that correlate with the behaviour of the density of modes.

## 1. Introduction

The properties of quasicrystals [1, 2] have aroused considerable interest since Shechtman *et al* [3] observed the long-range aperiodic arrangement of atoms in AlMn alloys. The concept of quasicrystals can be extended to other physical systems such as dielectric structures with feature size at the length scale of a micrometre or less, which are often called photonic microstructures. Periodic structures of this type, or photonic crystals, have attracted attention because of their potential application in the control of the propagation of electromagnetic radiation [4]. In particular, the spectrum of electromagnetic modes of such structures can possess gaps, photonic bandgaps, analogous to the gaps in the electronic energy eigenvalues of an insulator or semiconductor. However, such gaps are not easy to achieve for all field polarizations and all directions of propagation.

Photonic quasicrystals are of interest because a pseudogap, or near-vanishing minimum in the density of all modes, might be more readily achieved for all propagation directions in such structures as a result of their high degree of rotational ‘symmetry’. Indeed, a ‘sizeable spectral gap’ has been predicted theoretically for a two-dimensional photonic structure defined by the periodic repetition of a ‘supercell’ with local octagonal quasismmetry [5]. In addition, photonic quasicrystals provide a vehicle for studying quasicrystals in general. Photonic microstructures can provide a number of advantages in the investigation of the physical properties of a quasicrystal-like system because the structure can be designed to study particular phenomena and

can be investigated by well developed optical techniques [6].

Here we report a study of the optical diffraction properties, optical eigenmode spectrum and light transmission of a simple two-dimensional photonic quasicrystal. We begin by presenting the experimental diffraction pattern of the structure and show that it is consistent with simple optical diffraction theory. However, the diffraction properties of the structure and its theoretical interpretation also suggest an effective and straightforward method of describing the electromagnetic modes without introducing a supercell [5], rational approximant [7,8] or other aspects of periodicity into the model. Finally we calculate the transmission of light through the structure and compare the transmission spectrum and calculated band structure of our model system.

The structure considered is essentially a two-dimensional Penrose-tiled [9] dielectric slab, where the tiles are two kinds of rhombus: a thin tile (with vertex angles of 36° and 144°) and a fat tile (72° and 108°), as illustrated in figure 1(a). The experimental and model structures are formed by air cylinders which are positioned at the vertices of the tiles, as shown in figures 1(b) and (c).

The material and design of the structure used in the diffraction experiment was chosen to provide a simple experimental set-up. The design of the model system for the investigation of the band structure is different from the experimental one, in order to provide the most pronounced bandgap effects.

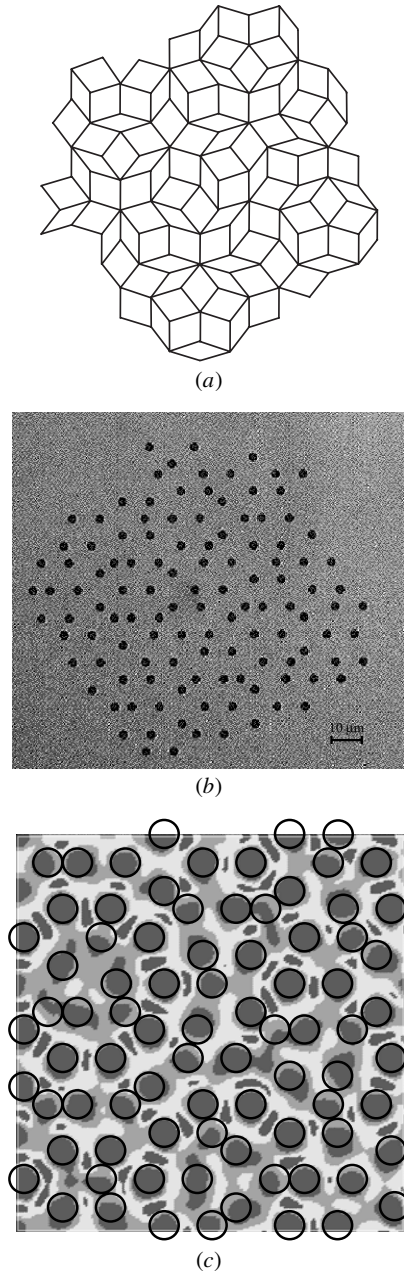


**Figure 1.** (a) Penrose tiling with thin and thick tiles. (b) Microphotograph of the sample, used in the diffraction experiment. (c) Schematic view of the original structure with cylinders positioned at the vertices of the tiles (black circles) and the reconstruction obtained via a back Fourier transform (greyscale) using 301 Fourier coefficients. Darker shading corresponds to the air cylinders, lighter to regions of surrounding material. It can be seen that even with such a small number of plane waves the original structure can be reasonably well represented.

## 2. Diffraction pattern

The experimental sample (see figure 1(b)) was fabricated using electron-beam lithography. The tile side is  $10 \mu\text{m}$  and the hole diameter is about  $3 \mu\text{m}$ . The quartz sample was first coated with 30 nm of titanium, then with a 900 nm layer of UV3 resist. After patterning, the air cylinders were etched using  $\text{CHF}_3$ . The depth of the cylinders was about

700 nm. Finally, the titanium coating was removed using high-field evaporation. The size of the patterned area is about  $120 \times 110 \mu\text{m}^2$  and contains 121 cylinders.

An He-Ne laser with a Gaussian shaped beam and a wavelength of 633 nm was collimated to provide a beam diameter of about  $130 \mu\text{m}$ , matching the size of the patterned area. The laser beam was incident normal to the sample, thus leading to the appearance of the diffraction pattern on the screen, placed 24 cm behind the sample (see figure 2(a)).

Note that although the experiment is carried out on a finite system with only 121 cylinders the pattern is remarkably similar to that reported for essentially infinite atomic quasicrystals [1], and also agrees with our theoretical predictions. The pattern possesses tenfold rotational symmetry, and contains a series of spots of different intensity, surrounding the central undiffracted beam. These spots can be associated with vectors in the reciprocal space which we call ‘reciprocal vectors’ (RVs).

In contrast to the case of a periodic crystal, the indexing of the diffraction pattern of aperiodic quasicrystals is not a trivial task, due to the self-similarity of the structure. The RVs of a periodic structure form the periodic reciprocal lattice and we can always find a set of primitive RVs of minimal magnitude whose linear combinations generate the entire reciprocal lattice. However, in aperiodic quasicrystals the RVs densely fill all reciprocal space, and it is not possible to choose any RVs of minimal magnitude. Nevertheless, it turns out to be convenient to choose some basic RVs that correspond to relatively intense peaks in the diffraction pattern, and have magnitudes that are related to the inverse of certain lengths in the structure, such as a tile side [2].

Figure 2(b) shows a photograph of the diffraction pattern of the experimental structure, with only three series of the most intense peaks visible. The magnitude and orientation of the RVs of the internal series correspond to the inverse of half the long diagonal of the thin tile. Similarly, the middle series corresponds to half the long diagonal of the thick tile and the external series corresponds to half of that tile side length.

We choose the RVs for the internal series of spots to form a basic set which we denote by  $\pm \mathbf{F}_i$  ( $i = 1, \dots, 5$ ), where

$$\mathbf{F}_1 = (1, 0) = (10000)$$

$$\mathbf{F}_2 = (\cos(\pi/5), \sin(\pi/5)) = (01000)$$

$$\mathbf{F}_3 = (\cos(2\pi/5), \sin(2\pi/5)) = (00100)$$

$$\mathbf{F}_4 = (\cos(3\pi/5), \sin(3\pi/5)) = (00010)$$

$$\mathbf{F}_5 = (\cos(4\pi/5), \sin(4\pi/5)) = (00001).$$

In the above equations, the vectors are expressed in both conventional two-dimensional Cartesian coordinates and a symbolic five-dimensional vector notation. The magnitude of each  $\mathbf{F}_i$  is related to the tile side length  $d$  as  $|\mathbf{F}_i| = 2\pi/(d \cos(\pi/10)) \approx 1.051 \times 2\pi/d$ . In the subsequent discussion we use  $|\mathbf{F}_i|$  as the unit of length in the reciprocal space. When we have chosen the basic set of RVs, it is possible to index the entire diffraction pattern. The intensities of the diffraction peaks related to the well pronounced different series, their index and related elements of the tiles defining the quasicrystal are shown in table 1. It can be seen that the most intense features are related to those RVs

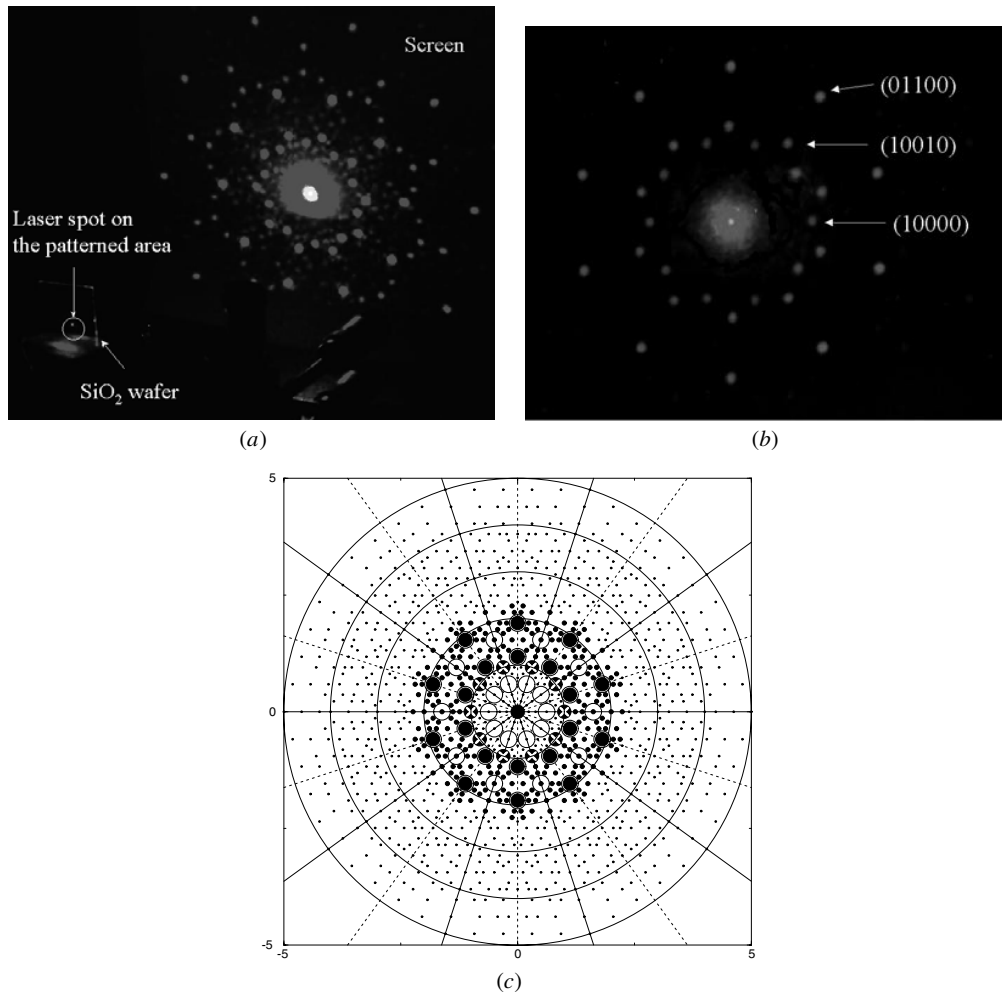


**Figure 2.** (a) General photograph of the experimental diffraction pattern. (b) Photograph of the most pronounced peaks on the experimental diffraction pattern and indexing of the diffraction pattern. (c) The map of the reciprocal lattice vectors is obtained using formula (1). The 301 RVs used in the back Fourier transform and band-structure calculation are shown by small and large solid circles. The RVs seen on the diffraction photograph are denoted by the large solid circles in a ring around the centre of the map. The dots represent the remainder of the 1200 RVs. The RVs  $\pm F_i$  are marked with white crosses. The RVs in the form  $\pm F_i \pm F_j$  for  $i \neq j$  are marked with open circles.

**Table 1.** Magnitudes of different Fourier coefficients of the Penrose structure and intensities of the diffracted beams.

RV	Magnitude	Intensity		Related intensity, normalized to the intensity of (10000)		The element of the tile, which can be associated with reciprocal vector
		Magnitude of Fourier coefficient	Power of the spots ( $\mu W$ )	Magnitude of Fourier coefficient	Power of the spots	
(00000)	0.000	0.416	1270	5.9	100	
(10001) <sup>a</sup>	0.618	0.018	Not pronounced	0.25	—	
(10000) <sup>a</sup>	1.000	0.070	6.7	1.00	1.00	Half of the long diagonal, thin tile
(10010)	1.176	0.065	8.3	0.92	1.23	Half of the long diagonal, thick tile
(10100) <sup>a</sup>	1.618	0.004	Not pronounced	0.06	—	Half of short diagonal, thick tile
(11000)	1.902	0.045	12.7	0.64	1.89	Half of the tile side
(11011) <sup>a</sup>	2.236	0.008	1.4	0.12	0.21	
(11100) <sup>a</sup>	2.618	0.019	1.6	0.27	0.24	
(11110)	3.078	0.022	1.8	0.31	0.27	Half of the short diagonal, thin tile

<sup>a</sup> RVs which are oriented as basic RV  $F_i$ .

which can be represented as ‘symmetric’ linear combinations with small coefficients of the basic RVs, such as (10000), (10010), (11000), etc. However, there are exceptions to this rule, such as the diffraction spot corresponding to RV (10100), which has very small intensity. It can also be seen that the strongest diffraction spots corresponds to two kinds of direction: either a basic set—(10000), (11011), (11100), or 18° off—(10010), (11000), (11110). The intensities of the peaks rapidly decrease as the number of basic RVs used increases, or with departure from the two directions specified above.

The entire diffraction pattern consists of a countable hierarchy of sharp Bragg diffraction peaks of different intensities, which densely fill all reciprocal space. However, the dominance of certain diffraction peaks suggests that, in practice, the spatial distribution of the dielectric constant  $\varepsilon(\boldsymbol{\rho})$  of the quasicrystal can be quite well represented in the form of a Fourier-like series:

$$\varepsilon(\boldsymbol{\rho}) = \sum_{\mathbf{G}_i} \chi(\mathbf{G}_i) \exp(i\mathbf{G}_i \boldsymbol{\rho}), \quad (1)$$

where  $\chi(\mathbf{G}_i) = \int \varepsilon(\boldsymbol{\rho}) \exp(-i\mathbf{G}_i \boldsymbol{\rho})$ , and the sum involves a limited number of vectors  $\mathbf{G}_i$  in reciprocal space, which are RVs of the type discussed above. The intensity of the diffraction spot corresponding to a particular  $\mathbf{G}_i$  is determined by the magnitude of the Fourier coefficient  $\chi(\mathbf{G}_i)$  in the Fourier transform of the spatial dependence of the dielectric constant of the structure. Because the magnitude of the coefficient  $\chi(\mathbf{G}_i)$  for the RVs of different series are sufficiently different, we need to employ only a limited number of RVs in order to provide a satisfactory representation of the structure. Note, however, that in quasicrystals RVs fill all reciprocal space, thus making the problem of Fourier representation of the spatial dependence of dielectric constant in a quasicrystal into a fractal description.

### 3. Band structure

A number of procedures for the calculation of the band structure of photonic *crystals* are well established [10]. Consider a two-dimensional photonic structure, comprising cylinders oriented along the  $z$ -axis and with the dielectric constant  $\varepsilon(\boldsymbol{\rho}) = \varepsilon(e_x x + e_y y)$  defined as a function of the two Cartesian coordinates  $x$  and  $y$ . An electromagnetic field propagating in the  $x$ - $y$ -plane can be represented as a superposition of fields with two independent polarizations: the  $H$ -polarization (with the magnetic field oriented parallel to the cylinders and field components  $(E_x, E_y, H)$ ) and the  $E$ -polarization (with the electric field oriented parallel to the cylinders and field components  $(H_x, H_y, E)$ ).

In the case of the  $H$ -polarization, the electromagnetic field component  $H$  varying with the frequency  $\omega$  must satisfy the wave equation

$$\frac{\partial}{\partial x} \left( \frac{1}{\varepsilon} \frac{\partial H}{\partial x} \right) + \frac{\partial}{\partial y} \left( \frac{1}{\varepsilon} \frac{\partial H}{\partial y} \right) + \frac{\omega^2}{c^2} H = 0. \quad (2)$$

To solve this equation we make a Fourier expansion of  $\varepsilon^{-1}(\boldsymbol{\rho})$  and  $H(\boldsymbol{\rho})$  such that

$$\frac{1}{\varepsilon(\boldsymbol{\rho})} = \sum_{\mathbf{g}_i} \tilde{\varepsilon}(\mathbf{g}_i) \exp(\mathbf{g}_i \boldsymbol{\rho}) \quad (3)$$

$$H(\boldsymbol{\rho}, \omega) = \sum_{\mathbf{g}_i} A(\mathbf{k}, \mathbf{g}_i) \exp((\mathbf{k} + \mathbf{g}_i) \boldsymbol{\rho}) \quad (4)$$

where the  $\mathbf{g}_i$  are the reciprocal lattice vectors of the crystal and  $\mathbf{k}$  is the two-dimensional wavevector of the wave in the  $x$ - $y$  plane. Note that the field  $H$  has the form of a Bloch wave, and  $\mathbf{k}$  can always be chosen to lie in the first Brillouin zone of the reciprocal lattice.

When these expansions are substituted into (2) we obtain a system of linear equations for the coefficients  $A(\mathbf{k}, \mathbf{g}_i)$ :

$$\sum_{\mathbf{G}'_i} (\mathbf{k} + \mathbf{g}_i)(\mathbf{k} + \mathbf{g}'_i) \tilde{\varepsilon}(\mathbf{g}_i - \mathbf{g}'_i) A(\mathbf{k}, \mathbf{g}'_i) = \frac{\omega^2}{c^2} A(\mathbf{k}, \mathbf{g}_i). \quad (5)$$

Equation (5) has the form of a standard eigenvalue problem with a symmetric matrix, which can be solved numerically to obtain the photonic band structure  $\omega(\mathbf{k})$  and corresponding mode field for any value of  $\mathbf{k}$ . The band structure of the  $E$ -polarized modes can be obtained in a similar fashion [10].

In other words, the dispersion relations for photonic *crystals* can be obtained if we have the spatial distribution of dielectric constant and the electromagnetic field of the eigenmode expressed in the form of a Fourier series.

We now propose that the spatial variation of the electromagnetic field of eigenmodes of quasicrystal should reflect the spatial dependence of the dielectric constant in the structure, and therefore can be represented as a Fourier-like series. Furthermore, it is suggested that we can obtain a good representation of the dispersion relations for the quasicrystal photonic eigenmodes by using the Fourier-like series of equation (1) in place of a true Fourier series in the theory of crystals described by equations (2)–(5).

Therefore to calculate the modes of photonic quasicrystals it is necessary to choose the appropriate set of RVs  $\mathbf{G}_i$ , rather than the reciprocal lattice vector  $\mathbf{g}_i$  in the case of a crystal. The  $\mathbf{G}_i$  should be such that they:

- are related to the strongest Fourier coefficients describing the distribution of the dielectric constant in the quasicrystal;
- cover the reciprocal space with the appropriate density, in order to describe the possible distribution of the electromagnetic field of the photonic eigenmodes;
- possess the rotational symmetry of the diffraction pattern.

The practicalities of the numerical calculation require that the number of RVs is limited. Nevertheless, the procedure used to generate such a set should be seen to lead, in the limit of including all the RVs, to the accurate integral Fourier representation of the dielectric constant (and spatial distribution of the field).

The straightforward way to choose the set of RVs for such a Fourier representation, is to take different linear combinations of the basic RVs with integer coefficients.

The set of RVs which satisfy the above-mentioned criteria is given by the formula

$$\mathbf{G}_m = \sum_{\substack{i=1,5 \\ k_i=1,2,3,4,5 \\ j_i=-1,0,1}} j_i \mathbf{F}_{k_i}. \quad (6)$$

Equation (6) gives the 1200 different scattering vectors, shown in figure 2(c), 80 of which have a magnitude less than unity. Continuation of this process would eventually give points filling all reciprocal space in a countable manner. For example, taking  $j_i$  from  $-2$  to  $2$ , one obtains 9200 different RVs.

The map of RVs in figure 2(c) shows multiple self-similarities [11–13]: outer sets of RVs can be obtained by inflation of the inner sets, and *vice versa*. As has been observed in quasicrystals [1] the magnitudes of RVs of different series can be related using the golden mean  $\tau = 1.618\dots$ . For example,  $|(10100)|/|01000| = \tau$ ,  $|(01100)|/|10010| = \tau$ ,  $|(10001)|/|00100| = \tau - 1$  etc.

In the case of *crystals*, the dispersion curves are periodic in reciprocal space, and the entire band structure is defined by the band structure inside the first Brillouin zone. Although *quasicrystals* do not possess a Brillouin zone, it is possible to formally construct the analogue of the Brillouin zone, the decagon in reciprocal space defined by the lines bisecting the basic RVs  $F_i$ , which is the so-called pseudo-Jones zone. It is believed that the properties of quasicrystals [7, 8] (such as indications of a bandgap) can be obtained by the investigation of band structure only inside the pseudo-Jones zone. Fourier coefficients, related to RVs of magnitude less than unity, have small magnitude and are not pronounced in the experimental diffraction pattern, and in the first stage of the calculation we neglect them. The solid curves in figure 3 show the calculated bands for the *H*-polarized modes along symmetry directions in the pseudo-Jones zone, together with the associated density of modes derived from the entire area of the zone. The calculations were performed using 301 Fourier coefficients to represent the electromagnetic field and inverse dielectric constant (as shown in figure 2(c)), which provides an accuracy of about 3% for the frequency of the lowest band. It can also be seen that such a small number of RVs provides a fair representation of the dielectric constant in the quasicrystal (see figure 1(c)). Note that there is a complete gap in the band structure near a frequency of 0.3 (in units of  $c/d$ , where  $c$  is the light velocity), which originates from the Bragg reflection of electromagnetic waves associated with the RVs  $F_i$ .

When an electromagnetic wave interacts with a spatially varying medium with Fourier coefficients corresponding to certain RVs, its wavevector can be changed by one RV or by any combination of RVs. In first order, the efficiency of this scattering is proportional to the Fourier coefficient of the RV. However, even if the Fourier coefficient related to some RV is zero, such scattering can take place in higher orders, and this scattering can produce features in the band structure and density of modes. Due to the smaller efficiency of higher-order scattering this should give only a minor contribution to the physical properties of the system.

We achieved convergence of the band structure and density of modes by taking more and more plane waves with magnitude greater than unity. However, it is interesting to consider the influence of RVs of magnitude less than the  $F_i$ . The dotted curve in figure 3 shows the band structure calculated taking into account the RVs of the type (10001), which have magnitude  $0.618\dots$ . The inclusion of these RVs results in the formation of a ‘minigap’ in the bands,

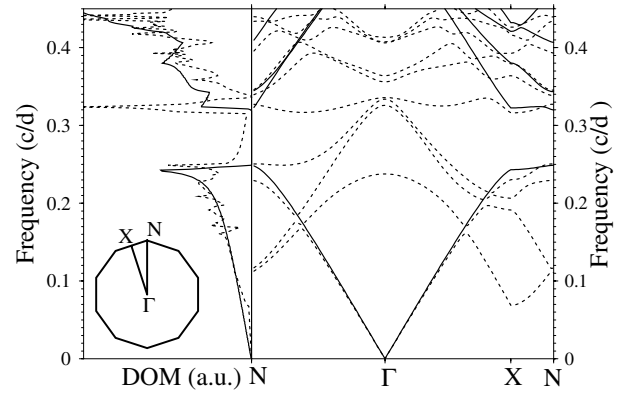


**Figure 3.** Results of band-structure calculations taking into account RVs of small magnitude. Dispersion curves and density of modes for *H*-polarization are calculated using 301 Fourier coefficients and plane waves (solid curve). Corresponding results calculated using an additional ten plane waves of smaller magnitude such as (10001) (dotted curve), see figure 2(b). Inset: symmetry points of the pseudo-Jones zone.

and related dips and spikes in the density of modes. They also lead to additional folding of the bands. However, the most significant feature is the appearance of allowed states inside the gap. These modes are characterized by a small wavevector and can be considered to be due to diffraction from the larger-scale elements of the (self-similar) quasicrystals.

In quasicrystals the RVs actually fill all reciprocal space [14, 15] and each can cause Bragg reflection and the appearance of minigaps, folding of branches and spikes in the density of modes like those of the RV of magnitude  $0.618\dots$ , although with varying strength. The effect on the band structure and the density of modes is to make it of a fractal character. A similar effect has been reported in the density of states of quasicrystals [13]. Taking more and more RVs leads to the appearance of new branches, with increasing density. Ultimately, at any value of wavevector  $k$ , it will be possible to find an allowed mode arbitrarily close to any value of frequency. In effect, a state with any  $k$  and  $\omega$  is, in general, allowed in a *quasicrystal*. However, only a fraction of these states will significantly influence a particular physical process.

This point can be illustrated by the experimental diffraction pattern (figure 2(a)), where it is possible to find a diffracted beam propagating in any direction, but only a small number of spots dominate the pattern. Therefore, in practice the problem is not to carry out an exact determination of band structure, but to recognize the hierarchy of branches, and select the relevant part for the physical process under consideration. In considering the transmission spectrum of a photonic quasicrystal a particular question is which modes are propagating and which are localized or whether they have some other nature.

On the one hand, the modes can be characterized by wavevector  $k$ , but on the other hand at any frequency and wavevector they can be scattered with the change of  $k$  corresponding to an RV. We might expect that modes suffer multiple scattering to propagate slowly, dwelling in finite regions of space, and even being localized. The latter can

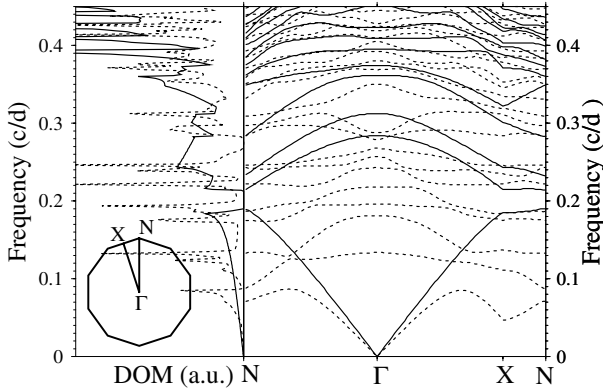


**Figure 4.** Results of band-structure calculation taking into account RVs of small magnitude. Dispersion curves and density of modes for  $E$ -polarization are calculated using 301 Fourier coefficients and plane waves (solid curve). Corresponding results calculated using an additional ten plane waves of smaller magnitude such as (10001) (dotted curve), see figure 2(b). Inset: symmetry points of the pseudo-Jones zone.

also explain the reduced conductivity in atomic quasicrystal alloys compared to the crystal phase of the same alloy [1].

Figure 4 shows the calculated band structure for the  $E$ -polarized wave. Although there are substantial differences from the case of  $H$ -polarized waves, there are also some effects common to both polarizations. Taking into account 301 plane waves, indicated in figure 2(c), one can obtain a gap, as in the case of  $H$ -polarized modes, but it is about one-third of the width and located at a frequency of about 0.2. Taking into account RVs of smaller magnitude, such as (10001), leads to a more substantial modification of the band structure and density of modes. A finite density of modes appears in the former gap, and an additional region of depleted density of modes occurs in the frequency regions in the neighbourhood of 0.08, 0.15 and 0.27.

#### 4. Transmission of the light

We have also calculated transmission spectra for the photonic quasicrystal of figure 1(b) using a modified version of the publicly available code of Bell *et al* described in [16]. The calculations have been performed by a combination of the transfer matrix method and the multiple-scattering technique. This method facilitates calculation of the propagation of light through a structure with a two-dimensional spatial variation of the dielectric constant, with applied periodic boundary conditions on the lateral (left and right) boundaries of the structure shown inset in figure 5 [16].

The application of periodic boundary conditions to the quasiperiodic structure results in discontinuity of the quasicrystal on the boundary of the supercell under consideration. The defects in crystal structure may cause the localization of light, and substantially modify the transmission spectra. In particular, this can lead to the appearance of sharp peaks in the spectral dip originating from the photonic bandgap corresponding to the ideal photonic crystal.

Figure 5 shows the transmission spectra for  $H$ - and  $E$ -polarized light propagating along two different directions,

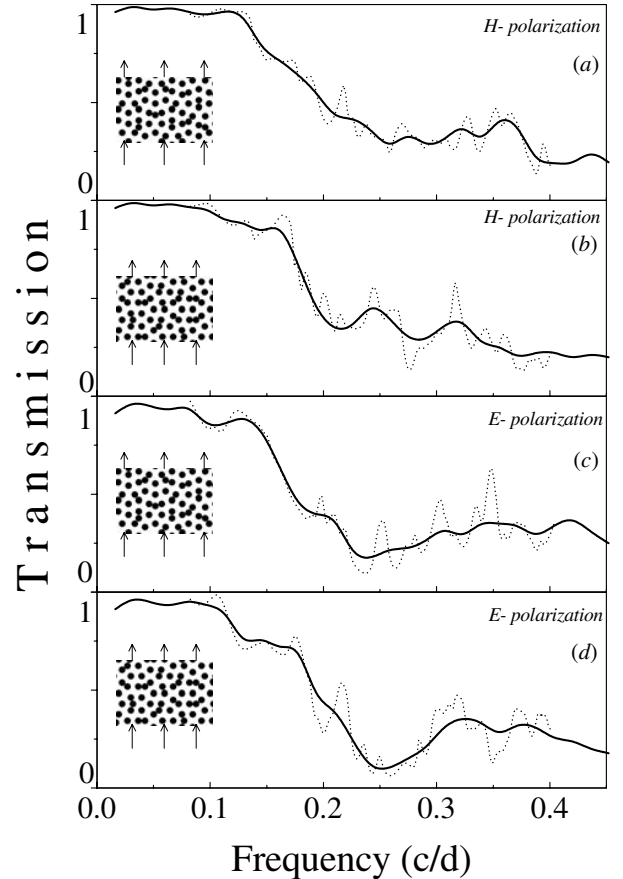


**Figure 5.** Calculated transmission spectra for  $H$ - and  $E$ -polarized waves, propagating along two different directions: (a)  $H$ -polarization, direction along  $F_i$ ; (b)  $H$ -polarization, direction  $18^\circ$  off  $F_i$ ; (c)  $E$ -polarization, direction along  $F_i$ ; (d)  $E$ -polarization, direction  $18^\circ$  off  $F_i$ . Insets show the ‘supercell’ used for modelling and direction of the light propagation.

along  $F_i$  (figures 5(b), (d)) and  $18^\circ$  off  $F_i$  (figures 5(a), (c)). The two types of supercell and the direction of the light propagation are shown in the inset. The dotted curves show the spectral dependence of the transmission coefficients for the relevant structures and polarizations. There are multiple spikes, probably associated with defect states, originating from the discontinuities of the Penrose structure on the front, rear and side boundaries. In order to exclude the influence of the defect states, we introduced some disorder (random variation of cylinder radii up to  $\pm 10\%$ ) into the structure, calculated transmission spectra for these different disorder configurations and then averaged the transmission spectra. Such a procedure allows us to exclude the influence of disorder and retain the spectral features caused by the regular ordering of photonic microstructure [17]. The resulting averaged transmission spectra are shown by the solid curves.

The spectra for  $E$ -polarized waves exhibit a broad but distinct minimum in the frequency region from 0.2 to 0.3, which corresponds to the gap in the density of modes in figure 4. The  $H$ -polarized spectra show relatively shallow double minima in the same region. However, in all cases the connections between features in the density of modes and

features in the transmission spectra are not as clear as in the case of periodic photonic *crystals*.

## 5. Conclusion

The distribution of matter in quasicrystals can, in practice, be well described using a rather small number of Fourier coefficients. The Fourier coefficients of largest magnitude are related to RVs obtained by taking a linear combination of a set of RVs associated with intense spots in the structure's diffraction pattern.

Quasicrystals possess a density of modes in the pseudo-Jones zone, which has fractal structure and is depleted around the frequency defined by the strongest Fourier coefficients. Inclusion of modes outside the pseudo-Jones zone increases the density of modes in the depleted region.

There is a discernible increase in the attenuation of waves around the frequencies corresponding to the depleted density of modes, but the effect is much weaker than in the bandgap of photonic crystals.

## Acknowledgments

Thanks are due to the EPSRC, who funded this work under grant awards GR/L 73159 and 73258, and to Professor M Burt for useful discussions.

## References

- [1] Janot C 1994 *Quasicrystals: A Primer* (New York: Oxford University Press)
- [2] Janssen T 1998 *Phys. Rep.* **168** 55
- [3] Shechtman D, Blech I, Gratias D and Canh J W 1984 *Phys. Rev. Lett.* **53** 1951
- [4] Joannopoulos J D, Meade R D and Winn J N 1995 *Photonic Crystals: Molding the Flow of Light* (Princeton, NJ: Princeton University Press)
- [5] Chan Y S, Chan C T and Liu Z Y 1998 *Phys. Rev. Lett.* **80** 956
- [6] Krauss T F, De La Rue R M and Brand S 1996 *Nature* **383** 699
- [7] Carlsson A E 1993 *Phys. Rev. B* **47** 2515
- [8] Sabiryanov R F and Bose S K 1994 *J. Phys.: Condens. Matter* **6** 6197
- [9] Penrose R 1974 *Bull. Inst. Math. Appl.* **10** 266
- [10] Plihal M and Maradudin A A 1991 *Phys. Rev. B* **44** 8565–71
- [11] Fu Xiujun, Liu Youyan, Zhou Peiqin and Wichit Sritrakool 1997 *Phys. Rev. B* **55** 2882
- [12] Boudard M, deBoissieu M, Janot C, Heger G, Beeli C, Nissen H-U, Vincent H, Ibberson R, Audier M and Dubois J M 1992 *J. Phys.: Condens. Matter* **4** 10 149
- [13] Janot C 1997 *J. Phys.: Condens. Matter* **9** 1493
- [14] Levin D and Steinhardt P J 1984 *Phys. Rev. Lett.* **53** 2477–80
- [15] Bancel P A and Heiney P A 1986 *Phys. Rev. B* **33** 7917
- [16] Bell P M, Pendry J B, Martin Moreno L and Ward A J 1995 *Comput. Phys. Commun.* **85** 306–22
- [17] Vlasov Yu A, Kaliteevski M A and Nikolaev V V 1999 *Phys. Rev. B* **60** 1555